

# EFFECTS OF THE SEAFLOOR TOPOGRAPHY ON TSUNAMI GENERATION EXPLORED FOR THE MESSINA 1908 TSUNAMI THROUGH 2-D FINITE ELEMENT MODELING

**Alberto Armigliato and Stefano Tinti**

Department of Physics, Sector of Geophysics, University of Bologna  
Viale Berti Pichat, 8 – 40127 Bologna – Italy

E-mail: [armigliato@ibogfs.df.unibo.it](mailto:armigliato@ibogfs.df.unibo.it), [steve@ibogfs.df.unibo.it](mailto:steve@ibogfs.df.unibo.it)

## ABSTRACT

We investigate the perturbations introduced by the local topography on the coseismic displacements induced by the December 28, 1908 Messina Straits (southern Italy) earthquake and the consequences for the generation mechanism of the triggered tsunami, which is the last catastrophic event of this kind to have hit the Italian coasts. The theoretical approach was recently introduced by Tinti and Armigliato (2002a, 2002b). It allows for the computation of coseismic deformations in homogeneous 2-D domains with arbitrary topography of the free surface. The solving algorithm is based on a two-step procedure using both analytical results, valid for a homogeneous space and a half-space bounded by a flat free surface (FFS), and a numerical code solving the equations of equilibrium of linear elasticity through a finite element (FE) scheme. The case of the Messina earthquake is very interesting, since large topographic and bathymetric gradients are involved in the source area. We compare the coseismic displacements computed through Okada's model (1992) valid for a FFS and through our approach, accounting for the effect of the actual topography. Very relevant effects are found both on the horizontal and on the vertical displacements, the former showing in general the greatest perturbations: in particular, a decisive role is found to be played by the position of the fault relative to the local topographic shape. Consequently, the tsunami generation mechanism, which strongly depends on the coseismic deformation of the seafloor, is expected to be seriously affected by the local topographic/bathymetric conditions.

## INTRODUCTION

It is commonly accepted that the generation mechanism of earthquake-induced tsunamis is related to the sudden displacement of the seafloor induced by the seismic shock: in particular, the initial sea surface perturbation is assumed to coincide with the vertical coseismic movement due to faulting. Hence, the key problem becomes that of adopting a reliable model for the computation of the coseismic deformation of the ocean bottom. The simplest and most widely adopted approach is that of modelling the Earth's crust as a homogeneous and isotropic elastic half-space bounded by a flat-free surface (FFS). For this case a complete set of analytical formulas is available for the displacement and stress fields induced by arbitrary double-couple point sources as well as by rectangular faults. A major drawback of the application of this model to the tsunami generation problem is that the seafloor topography is completely neglected. This aspect is particularly critical when the seismic sources are very close to or even intersect the coastlines and when relevant topographic structures like escarpments or grabens are involved, which is the typical scenario for the tsunami source regions in the Mediterranean sea. Approximate algorithms (Tanioka and Satake, 1996; Tinti and Armigliato, 1999) have already been proposed to try to overcome this problem. The basic idea is to simulate the effect of a non-flat bathymetry by taking into account also the horizontal movement of the sea bottom and by computing the correction it adds to the vertical displacement. This kind of approach, though useful for rough estimates of the effect of an

irregular bathymetry, is not correct since it doesn't allow for the computation of the coseismic displacements exactly on the points belonging to the bathymetric relief. This goal can be accomplished by means of a numerical code we developed recently (Tinti and Armigliato, 2002a, 2002b), which solves the equilibrium equations of linear elasticity in two dimensions through a finite element scheme. The approach is here applied to compute the coseismic displacements along selected 2-D cross sections intersecting the Messina Straits in southern Italy, where the last catastrophic tsunami hitting the Italian coasts was generated by the December 28, 1908,  $M=7.2$  earthquake. By adopting some of the most reliable fault models proposed in the literature for this earthquake, we compare the results accounting for the seafloor topography with those obtained through the FFS analytical formulas and the approximate algorithms cited above, and we discuss the consequences for the tsunami generation process.

### **THE MESSINA STRAITS AND THE DECEMBER 28, 1908 EARTHQUAKE AND TSUNAMI**

The Messina Straits, together with southern Calabria and eastern Sicily, is among the most earthquake-prone areas in Italy. Its very high seismicity rate, one of the highest in the whole Mediterranean, is directly imputable to the complicated tectonic setting of the region, which is dominated by a major normal fault belt running more or less continuously along the inner side of the Calabrian Arc, the Messina Straits and the Ionian coasts of Sicily (e.g. Monaco and Tortorici, 2000). A large number of the normal faults forming the belt are placed partially or totally offshore, and are then potentially tsunamigenic. Tsunami catalogues (e.g. Tinti and Maramai, 1996) report several strong earthquake-generated tsunamis attacking the coasts of southern Calabria and eastern Sicily in historical times. The December 28, 1908 earthquake in the Straits of Messina triggered the most recent one. The shock, which took place at 4:20 GMT and had an estimated magnitude  $M_S = 7.2$ , caused the almost complete destruction of the coastal towns of Messina and Reggio Calabria and very high damage in an area as large as 6000 km<sup>2</sup>. The earthquake reached degree XI in the MCS intensity scale and claimed a dramatically high number of casualties (80,000 according to Boschi et al., 2000). The violent tsunami that followed further increased both the level of destruction and the number of casualties. In most places the first observed sea movement was a withdrawal: in some localities the sea retreated for about 200 m (Tinti and Maramai, 1996). Then the sea flooded the coast with at least three big waves, the second of which was the most destructive one, at least inside the Straits. A post-event survey (e.g. Platania, 1909) allowed to estimate damage, flooding and run-up: incidentally, the 1908 tsunami is the only event of this type occurred in Italy for which an extensive dataset of measured penetration distances and run-ups are available. In the upper panel of Figure 1, the black dots indicate coastal stations in which observations and measurements were collected: some of the measured run-ups are also reported.

Despite the conspicuous amount of measured data available for both the earthquake (macroseismic and levelling data, seismic recordings) and the tsunami, an agreement on the causative fault has not been achieved so far. Anyhow, here we are not going to pay any attention to the problem of the identification of the parent fault: the interested reader can refer, for example, to the introduction of the paper by Amoruso et al. (2002). Rather, we are going to adopt one particular fault model proposed in the literature and to investigate the effect of the topography/bathymetry of the Messina Straits area on the 2-D coseismic displacements induced by the fault. The surface projection of the chosen source used here is sketched as a black-bordered rectangle in the lower panel of Figure 1. It was first introduced by Capuano et al. (1988) and De Natale and Pingue (1991) on the basis of the inversion of levelling data and

it was later adopted by Tinti and Armigliato (2000, 2001) as a starting point to perform tsunami numerical simulations, and in particular to invert tsunami run-up observations and to compare results vs levelling data. The main conclusions obtained in the studies by Tinti and Armigliato (2000, 2001) are that 1) it is difficult to find a single source matching simultaneously both tsunami and levelling data, and 2) a sensible improvement on the computed run-up distribution is obtained if the original fault by Capuano et al. (1988) is extended or shifted to the south. This last conclusion has recently been confirmed by the results obtained by Amoruso et al. (2002) through joint inversion of seismic and levelling data.

## **MODELLING THE TOPOGRAPHY EFFECT ON COSEISMIC DISPLACEMENTS: THEORETICAL APPROACH**

The theoretical model we adopt has been recently introduced by Tinti and Armigliato (2002a, 2002b) and applied to three different earthquake sequences occurred along the Alpine and the Apennine chains, Italy. The model allows computing coseismic displacements in 2-D purely elastic and homogeneous domains bounded by free surfaces that can assume any irregular shape. It can be defined as a two-step hybrid approach, in that the solution is obtained as the sum of two distinct terms, computed in two distinct steps and with different techniques. The first term reflects the contribution of the seismic source (source term, ST), modelled as a distribution of double-couples of forces: it is computed through the classic analytical formulas valid for faults embedded in homogeneous elastic unbounded spaces. The second term is the correction that must be added to ST when a free surface is introduced. The correction, which is found to be particularly relevant for shallow faults characterized by shallow dip angles, can be computed in analytical form only when the free surface is flat (e.g. Okada, 1992). In all the other cases, only approximate solutions can be determined by means of analytical and/or numerical techniques. In our approach, the free surface correction (FSC) term is computed through an original finite element (FE) code, which solves the equations of elastic equilibrium in 2-D in the plane-strain approximation. The final solution is obtained as the sum of the analytical results for ST and of the numerical solution for FSC.

It is worth recalling here that our hybrid approach presents both a drawback and a relevant advantage on the models based exclusively on the FE technique (see Tinti and Armigliato, 2002a, 2002b for further details). The drawback is that our method is limited to perfectly homogeneous domains. On the other hand, pure FE codes must include explicitly the fault on the computational mesh and prescribe the displacements on its nodes as known boundary conditions. While it is possible to determine the displacements related to ST analytically for any arbitrary free surface shape, it is not possible to compute FSC "a priori" when the free surface is not flat. In these cases, pure FE models cannot account for FSC, even in perfectly homogeneous domains. Conversely, the adoption of our two-step approach guarantees that both ST and FSC are correctly accounted for, even in presence of an irregular topography. Further, it is not necessary to introduce the fault into the FE mesh, which brings the interesting practical advantage that the same mesh can be used for faults with similar positions but different geometric and focal parameters.

## **APPLICATION TO THE 1908 EARTHQUAKE: RESULTS AND CONCLUSIONS**

The Messina Straits region is a particularly interesting test case for our model, as can be observed by looking at the lower panel of Figure 1. Here the topography of the studied area is

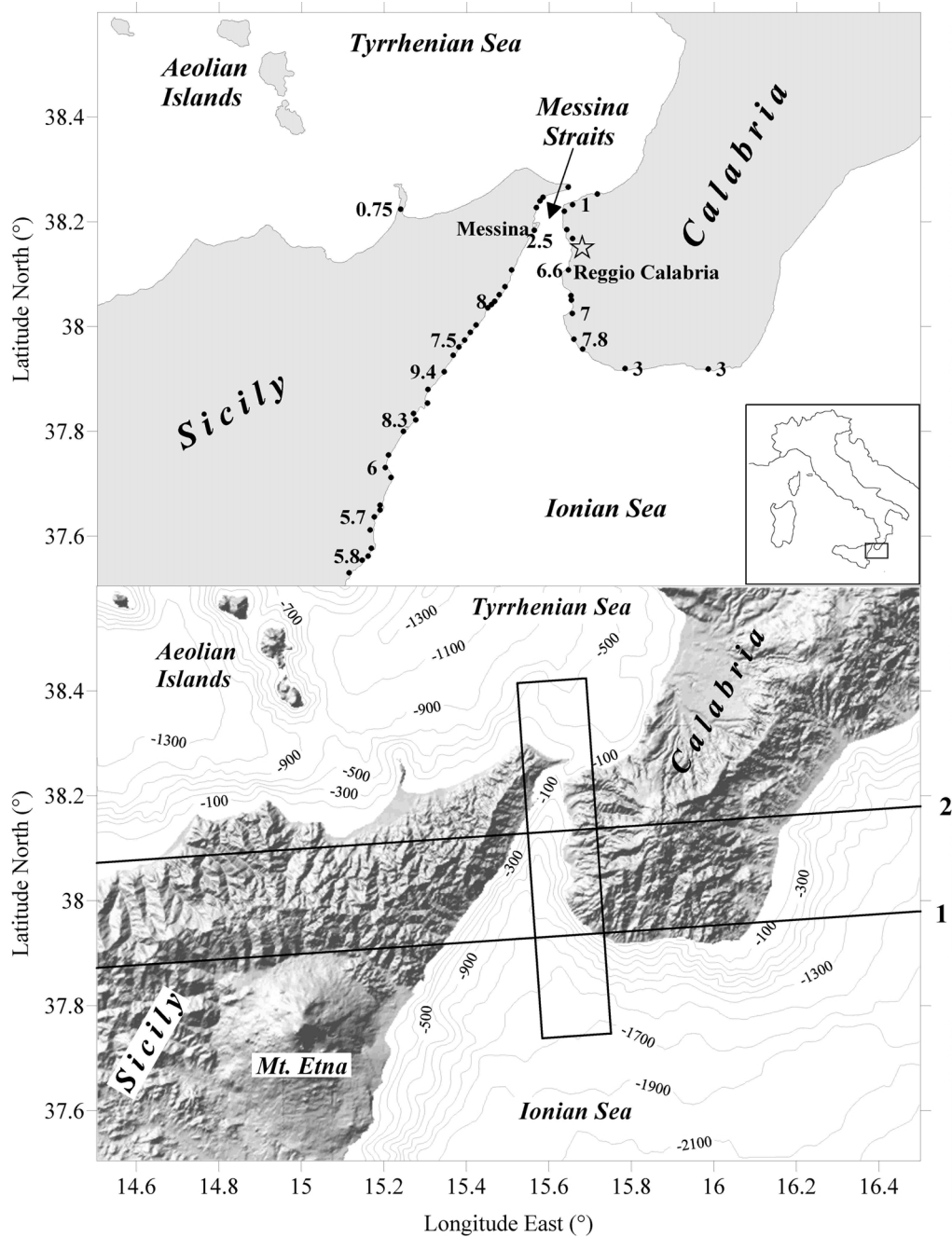


**Figure 1.** *Upper panel:* map of the Messina straits region hit by the December 28, 1908 earthquake and tsunami. Black dots indicate localities for which tsunami run-up observations are available (Tinti and Giuliani, 1983): only some of them (with values expressed in metres) are reported in the Figure. The star is the earthquake epicentre as defined by Boschi et al. (2000). *Lower panel:* topography (shaded relief) and bathymetry (contour map): depth labels are expressed in metres. The rectangle is the surface projection of the earthquake fault. Lines 1 and 2 are the profiles along which coseismic displacements are computed.

plotted: abrupt changes in the free surface shape can be appreciated even over small distances, with positive values as high as 2500 m a.s.l. in the mountain range of south Calabria and bathymetric depths exceeding 1500 m. Note in particular that the surface projection of the fault we adopt in this study lies in a domain characterized by very rapid topography variations. Hence, it is reasonable to expect that neglecting the real topography/bathymetry in this case

can produce biased results for the computed surface coseismic displacements. Since the initial tsunami elevation is generally assumed to coincide with the coseismic deformation of the seafloor, incorrect modelling of the tsunami generation process, and consequently of the tsunami propagation and impact on the coasts, could be a direct consequence. Our main goal here is to quantify the effect of the local topography on the coseismic deformation pattern and to compare the results with those obtained through the traditional analytical modelling involving FFS (Okada, 1992). Since our model is 2-D, we must perform our computations along vertical cross-sections: in this study we select the cross-sections along the lines numbered 1 and 2 in the lower panel of Figure 1. The topographic shapes along the two profiles are sketched in Figure 2, together with the position of the fault. Note that the horizontal and vertical axes have different scales, with the consequence that the dip angle and the width of the fault are highly distorted.

Two general comments arise from Figure 2. The first regards the definition of the depth of a fault. In cases like the Messina 1908 earthquake for which geodetic data are available, one possible way to retrieve the relevant geometric and focal parameters of the genetic fault is to invert the measured data through the FFS analytical models. This procedure requires that a reference elevation for the free surface be adopted, even in regions of highly variable topography. Unfortunately, in general no mention to this basic choice is made in the studies dealing with the computation of the fault parameters by geodetic data inversion. Let us take in consideration the particular case studied here, in which the upper border of the fault is defined to be 2 km deep. We chose to refer this depth to the  $z=0$  elevation, but the plots in Figure 2 clearly show that different choices are possible in principle. For example, the depth could be referred to the local elevation of the free surface, or to the average value of the topography along the geodetic path. Obviously, different choices could lead to significantly different results.

The second general comment is related to the previous one and is even more tricky. In the FFS models it is assumed that the upper border of the fault lies parallel to the FFS. By comparing

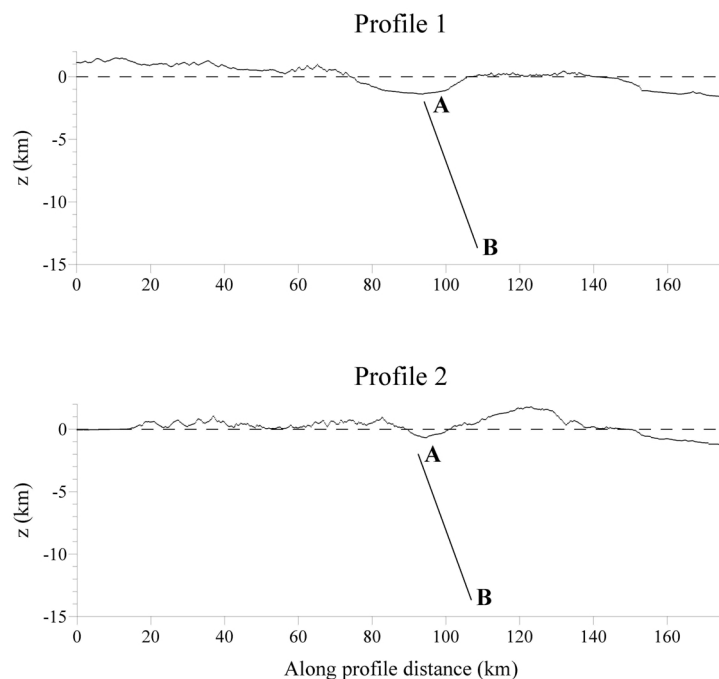


**Figure 2.** Surface topography along the profiles drawn in the lower panel of Figure 1. AB is the fault intersection with the vertical plane.

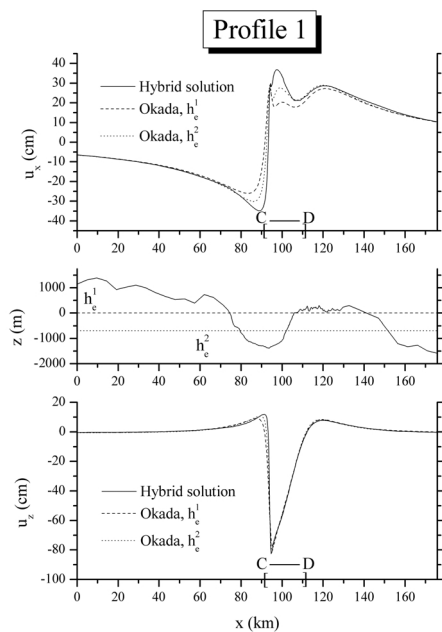


**Figure 3.** Coseismic displacements components  $u_x$  (upper panel) and  $u_z$  (lower panel) along the surface profile 1. Segment CD is the surface projection of the fault AB in Figure 2. The central panel shows the topographic relief and the two reference FFS elevations:  $h_e^1=0$ ,  $h_e^2=-693$  m. Square brackets show the interval used to compute  $h_e^2$ .

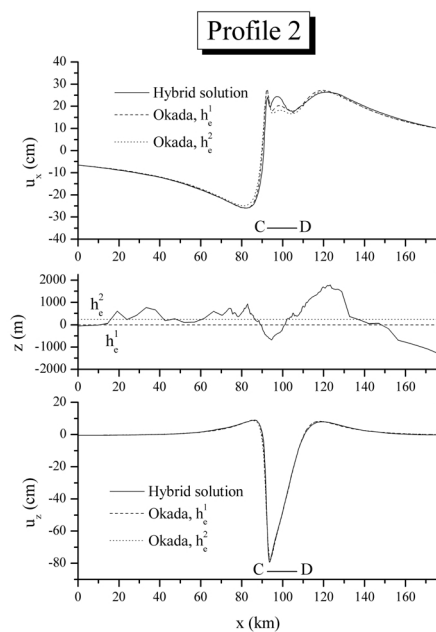


**Figure 4.** Same as Figure 3, but for profile 2. The two reference FFS altitudes are  $h_e^1=0$ ,  $h_e^2=237$  m.

the position of the fault along profiles 1 and 2 in Figure 2, we may observe that its upper border has different depths relative to the local topography depending on the position along the strike. Hence, if a uniform slip distribution is prescribed on the fault plane, we expect, at least locally, the surface displacements observed along profile 1 to be greater than those observed along profile 2. Another interesting consequence is that, when geodetic data are inverted to retrieve the slip distribution on a prescribed fault plane, the result could contain also the spurious effect due to the different local depths of the fault.

Figures 3 and 4 illustrate the surface displacements induced by the selected fault model along profiles 1 and 2, respectively. It is worth mentioning that the adopted fault is characterized by a width of 18.5 km, a dip angle of  $39^\circ$ , a depth of 2 km referred to the reference  $z=0$  level, and a normal mechanism with average slip of 1.5 m. Since we are working under the plane-strain approximation, the length of the fault is theoretically infinite. Starting from Figure 3, the upper and lower panels contain the curves relative to the horizontal ( $u_x$ ) and vertical ( $u_z$ ) displacement components, respectively. Solid lines indicate the results obtained through our hybrid technique, accounting for the topography effect, while the other two curves illustrate the displacements obtained through Okada's analytical formulae, valid for FFS. When computing the latter solutions, we must choose some sort of "equivalent" or "reference" flat level  $h_e$ : if we indicate with  $d$  the depth of the fault top with respect to the  $z=0$  plane,  $h_e + d$  will indicate the depth of the top of the reference Okada's fault. The two different choices adopted here for  $h_e$  are displayed in the central panel of Figure 3, together with the topography

along profile 1. The two choices for  $h_e$  correspond respectively to the "zero elevation" level ( $h_e^1=0$ ) and to the topography average value computed on the interval  $91.3 \text{ km} \leq x \leq 111.3 \text{ km}$  containing the source surface projection CD ( $h_e^2 = -693 \text{ m}$ ). As regards the displacement's vertical component  $u_z$ , the differences between the two solutions are quite significant only in a very narrow interval around the surface projection of the upper fault border. Both the positive and the negative peaks of the solution accounting for topography are amplified with respect to the analytical signals: this effect is a direct consequence of the fault being locally closer to the real free surface than to  $h_e^1$  and to  $h_e^2$ . The differences are even more evident in the upper panel of Figure 3, concerning the horizontal displacement  $u_x$ . Here the discrepancies are appreciable in a much wider interval, and are particularly relevant in correspondence of the projection of the upper part of the fault and to the left of its upper border. Like for  $u_z$ , large amplifications with respect to the FFS solutions are observed both for the positive and for the negative peaks of  $u_x$ .

Figure 4 shows the results obtained along profile 2. As in the previous case,  $h_e^1$  corresponds to the "zero elevation" level ( $h_e^1=0$ ), while  $h_e^2$  is chosen as the mean altitude computed over the entire profile ( $h_e^2 = 237 \text{ m}$ ). As may be seen, the discrepancies are much smaller than along profile 1. As regards the vertical displacement  $u_z$ , the three curves are almost superimposed, so that topography seems to add no relevant correction to this component. Some non-negligible differences are still visible in the horizontal signal  $u_x$ , and they are confined to the projection of the upper portion of the fault plane. It is possible to observe here the peculiar effects due to the shape of the topographic relief (central panel): with respect to the analytical signal computed for  $h_e^1$ , the curve accounting for topography shows a reduced positive peak in correspondence with the upper border of the fault (where the local topography is positive) and an amplified peak in correspondence with the central part of the fault projection, where the local topography is negative.

In conclusion, we may summarize the results obtained in this study in the following points, which are in agreement with the recent results presented by Tinti and Armigliato (2002a, 2002b) for Alpine and Apennine earthquakes:

- 1) The perturbations introduced by the local topography are mainly related to amplification/reduction effects with respect to the solutions computed for FFS.
- 2) The horizontal component  $u_x$  is the one on which topography induces the most evident perturbations. The greatest misfit is observed in correspondence with the surface projection of the fault and near its upper end.
- 3) The discrepancies on the vertical signals  $u_z$  are limited to a very narrow interval around the surface projection of the fault upper edge.
- 4) A key role is played by the position of the fault, and in particular of its upper edge, relative to the topographic shape.

Finally, the effects observed in the case of the Messina 1908 earthquake are expected to play a very important role in the tsunami generation mechanism. It has to be outlined that for more detailed investigations on this topic, a 2-D model like the one adopted here is not sufficient and a fully 3-D approach will be necessary.

## References

Amoruso A., Crescentini L., and Scarpa R., 2002: Source parameters of the 1908 Messina Straits, Italy, earthquake from geodetic and seismic data. *J. Geophys. Res.*, **107**.

- Boschi E., Guidoboni E., Ferrari G., Mariotti D., Valensise G., and Gasperini P., 2000; Catalogue of strong Italian earthquakes from 461 B.C. to 1997. *Annali di Geofisica*, **43**, 609-868.
- Capuano P., De Natale G., Gasparini P., Pingue F., and Scarpa R., 1988: A model for the 1908 Messina Straits (Italy) earthquake by inversion of levelling data. *Bull. Seism. Soc. Am.*, **78**, 1930-1947.
- De Natale G., and Pingue F., 1991: A variable slip fault model for the 1908 Messina Straits (Italy) earthquake by inversion of levelling data. *Geophys. J. Int.*, **104**, 73-84.
- Monaco C., and Tortorici L., 2000: Active faulting in the Calabrian arc and eastern Sicily. *J. Geodynamics*, **29**, 407-424.
- Okada Y., 1992: Internal deformation due to shear and tensile faults in a half-space. *Bull. Seism. Soc. Am.*, **82**, 1018-1040.
- Platania G., 1909: Il maremoto dello Stretto di Messina del 28 dicembre 1908. *Boll. Soc. Sism. Ital.*, **13**, 369-458 (in Italian).
- Tanioka Y., and Satake K., 1996: Tsunami generation by horizontal displacement of ocean bottom. *Geophys. Res. Lett.*, **23**, 861-864.
- Tinti S., and Armigliato A., 1999: Seismic displacements of non-flat sea floor in tsunami generation: application to the 1693 case in SE Sicily, Italy. In: *Proceedings of the International conference on Tsunamis*, Paris, 26-28 May 1998, 225-245.
- Tinti S., and Armigliato A., 2000: Tsunamigenic earthquakes. In: E. Boschi, G. Ekström and A. Morelli (Eds), *Problems in Geophysics for the New Millennium*, INGV-Editrice Compositori, 27-46.
- Tinti S., and Armigliato A., 2001: Impact of large tsunamis in the Messina Straits, Italy: the case of the 28 December 1908 tsunami. In: G.T. Hebenstreit (ed), *Tsunami Research at the End of a Critical Decade*, Kluwer Academic Publishers, 139-162.
- Tinti S., and Armigliato A., 2002a, A 2-D hybrid technique to model the effect of topography on coseismic displacements. Application to the Umbria-Marche (central Italy) 1997 earthquake sequence, *Geophys. J. Int.*, **150**, 542-557.
- Tinti S., and Armigliato A.; 2002b, Influence of topography on coseismic displacements induced by the Friuli 1976 and the Irpinia 1908 earthquakes (Italy) analyzed through a 2-D hybrid model. *J. Geophys. Res.* (submitted).
- Tinti S., and Giuliani D: 1983, The Messina Straits tsunamis of December 28, 1908: a critical review of experimental data and observations. *Il Nuovo Cimento*, Serie 1, **6C**, 429-442.
- Tinti S., and Maramai A., 1996: Catalogue of tsunamis generated in Italy and in Côte d'Azur, France: a step towards a unified catalogue of tsunamis in Europe. *Annali di Geofisica*, **39**, 1253-1299 (Errata Corrigé in *Annali di Geofisica*, **40**, 781).